

FERMILAB-PUB-99/259-T  
October 7, 1999

## STOP AND SBOTTOM SEARCHES IN RUN II OF THE FERMILAB TEVATRON

REGINA DEMINA

*Department of Physics and Astronomy  
Kansas State University  
Manhattan, KS 66506, USA*

JOSEPH D. LYKKEN and KONSTANTIN T. MATCHEV

*Theoretical Physics Department  
Fermi National Accelerator Laboratory  
Batavia, IL 60510, USA*

ANDREI NOMEROTSKI

*Physics Department  
University of Florida  
Gainesville, FL 32611, USA*

### Abstract

We estimate the Tevatron Run II potential for top and bottom squark searches. We find an impressive reach in several of the possible discovery channels. We also study some new channels which may arise in non-conventional supersymmetry models. In each case we rely on a detailed Monte Carlo simulation of the collider events and the CDF detector performance in Run I.

# 1 Introduction

For most of the next decade, the Fermilab Tevatron collider will define the high energy frontier of particle physics. The first stage of the Tevatron collider Run II, scheduled to begin in 2000, will deliver at least  $2 \text{ fb}^{-1}$  of integrated luminosity per experiment at 2.0 TeV center-of-mass energy; this is more than 10 times the luminosity delivered in previous collider runs at 1.8 TeV. Major upgrades of the CDF and D0 detectors are under way. Among other features, the detectors will have the ability to trigger on displaced vertices from bottom and charm decays using a precise microvertex detector.

Along with top physics, searches for supersymmetry (SUSY) are among the main priorities for Run II. The Minimal Supersymmetric Standard Model (MSSM) is an attractive extension of the Standard Model. On the one hand, it agrees with precision measurements and cannot be easily ruled out through indirect searches [1]. On the other hand, it is theoretically well motivated by various ideas about physics at very high energy scales – string theory, supergravity, grand unification. It also stabilizes the Higgs mass against radiative corrections, even though it does not provide the complete answer as to why the electroweak scale is so much lower than the Planck scale.

Currently, we have no idea which of the supersymmetric particles are the lightest and as such, more easily accessible at colliders. With all things being equal, however, the lightest stop  $\tilde{t}_1$  is a very good candidate for studying at the Tevatron. First, it is colored, and so its production cross section is much larger than that for sleptons, for example. Second, it is feasible that the stop is the lightest squark. This may be due for example to a large mixing angle  $\theta_t$  between the superpartners of the left-handed and the right-handed top quarks,  $\tilde{t}_L$  and  $\tilde{t}_R$  respectively, which form the lightest stop mass eigenstate:  $\tilde{t}_1 = \tilde{t}_L \cos \theta_t + \tilde{t}_R \sin \theta_t$ . Alternatively, the large top Yukawa coupling  $\lambda_t$  enters the renormalization group (RG) equations of the stop soft masses and tends to reduce them in comparison to the other squarks. We shall discuss each of these effects in more detail in Section 2.1. If the stop is the lightest of all squarks, its production at the Tevatron will be least suppressed by kinematics. Yet another motivation to look for a light stop is that it seems to be preferred for electroweak baryogenesis [2].

The purpose of this paper is to establish a basis for a systematic stop search in the

upcoming Run II at the Tevatron. We shall consider the most promising stop signatures in a variety of supersymmetric models. In each case, we shall discuss under what circumstances the stop can be light, what is the optimal search strategy, and what is the Tevatron reach.

In general, the typical SUSY signatures are determined by the nature of the lightest supersymmetric particle (LSP) and whether R-parity is conserved or not. Conservation of R-parity implies that all SUSY decay chains end up in the LSP, which is stable and leaves the detector. If the LSP is charge- and color-neutral, as can often be the case in both supergravity and gauge-mediated models of supersymmetry breaking, then a typical SUSY signature is the missing transverse energy  $\cancel{E}_T$ . A charged or colored stable LSP could lead to more exotic signatures (see, for example [3, 4, 5]). R-parity violating interactions [6] would allow the LSP to decay into Standard Model particles. For the purposes of this paper we limit ourselves to a class of SUSY models where R-parity is conserved and the LSP is charge and color neutral: i.e. it is either the lightest neutralino (as in supergravity mediated (SUGRA) models of SUSY breaking), or the gravitino (as in gauge mediated (GM) models).

The plan of the paper is as follows. In Section 2 we start with a review of the traditional searches for a light stop, which were motivated to a large extent by the minimal version (mSUGRA) of the SUGRA models. Therefore, in Section 2.1 we first describe the relevant part of the mSUGRA parameter space which can be explored via those analyses. Notice, however, that even though we choose to work within the framework of mSUGRA, our results are valid for a generic MSSM. In fact, each analysis only makes an assumption about the mass ordering of a few supersymmetric particles, and is not constrained to any particular mechanism of SUSY breaking. In Section 2.2 we summarize the assumptions and basic facts from Run I that were used in the analyses to follow. We then proceed to estimate the Run II projections for the Tevatron reach in light stop searches for the following three channels:  $\tilde{t} \rightarrow \tilde{\chi}_1^+ b$  (Section 2.3),  $\tilde{t} \rightarrow \tilde{\chi}_1^0 c$  (Section 2.4) and  $\tilde{t} \rightarrow \tilde{\nu} \ell^+ b$  or  $\tilde{t} \rightarrow \tilde{\ell}^+ \nu b$  (Section 2.5). We then depart from the mSUGRA framework, and consider the possibility of non-universal scalar masses at the unification scale. This may lead to a situation where the neutralino LSP is mostly higgsino-like, which will alter the light stop search strategy. Such a case is studied in Section 3, where we present the reach as a

function of the higgsino and stop mass. As the stop becomes increasingly degenerate with the LSP, the signals from direct stop production become lost and one has to look for stops among the decays of other sparticles, e.g. charginos. In Section 4 we consider decays of (possibly higgsino-like) charginos to stops. We devote Section 5 to sbottom searches, since in many respects the analysis is similar to some of the stop searches considered before. We delineate the relevant SUGRA parameter space and present Run II expectations. Finally, in Section 6 we translate our previous results for the case of light stops in GM models. We reserve Section 7 for our conclusions.

## 2 Traditional Stop Searches

In this section we discuss the relevant mSUGRA parameter space for the traditional stop searches. We then estimate the Run II sensitivity in these channels.

### 2.1 Review of the relevant mSUGRA parameter space

Most of the SUSY searches in the past have been performed within the SUGRA framework, where supersymmetry breaking, which takes place in a hidden sector, is communicated to the MSSM fields through gravitational interactions. The sparticle spectrum can be calculated in terms of the soft SUSY breaking parameters, which are in principle free inputs at the Planck scale  $M_P$ . In the minimal version of the SUGRA models (mSUGRA), it has become a custom to input the soft masses at the grand unification (GUT) scale  $M_{\text{GUT}}$  instead, and in addition one assumes universality among the scalar masses, the gaugino masses and the trilinear Higgs-sfermion-sfermion couplings. The mSUGRA parameter space therefore consists of only five parameters: a universal scalar mass  $M_0$ , a universal gaugino mass  $M_{1/2}$ , a universal trilinear scalar coupling term  $A_0$ , all defined at the GUT scale, as well as the ratio of the two Higgs vacuum expectation values  $v_u/v_d \equiv \tan \beta$  and the sign of the  $\mu$  parameter. One can readily identify which regions of this mSUGRA parameter space would be associated with a light stop, simply by inspection of the stop mass matrix

$$\mathcal{M}_{\tilde{t}} = \begin{pmatrix} M_{\tilde{Q}_3}^2 + m_t^2 + (\frac{1}{2} - \frac{2}{3} \sin^2 \theta_W) M_Z^2 \cos 2\beta & m_t(A_t + \mu \cot \beta) \\ m_t(A_t + \mu \cot \beta) & M_{\tilde{t}_R}^2 + m_t^2 + \frac{2}{3} \sin^2 \theta_W M_Z^2 \cos 2\beta \end{pmatrix}, \quad (1)$$

where  $M_{\tilde{Q}_3}$  ( $M_{\tilde{t}_R}$ ) is the soft mass parameter for the left-handed (right-handed) top squark,  $m_t$  is the top quark mass,  $M_Z$  is the  $Z$ -boson mass,  $\theta_W$  is the Weinberg angle and  $A_t$  is the soft trilinear  $\tilde{t}_L \tilde{t}_R H_u$  coupling. All parameters entering eq. (1) are to be evaluated at the low-energy scale (near the stop mass). In the mSUGRA model,  $A_t$  is most directly related to its boundary condition at the GUT scale,  $A_0$ , while  $M_{\tilde{Q}_3}$  and  $M_{\tilde{t}_R}$  have a dependence on both  $M_0$  and  $M_{1/2}$ . The  $\mu$  parameter is obtained from the condition that proper electroweak symmetry breaking reproduces the experimentally observed  $Z$ -boson mass. Notice the possibility of a large stop mixing:

$$\sin 2\theta_t \sim \frac{2m_t(A_t + \mu \cot \beta)}{m_{\tilde{t}}^2} \sim \frac{2m_t A_t}{m_{\tilde{t}}^2} \quad (\text{at moderate to large } \tan \beta). \quad (2)$$

If there were no such mixing, the stop masses would be roughly equal to the corresponding soft mass parameters  $M_{\tilde{Q}_3}$  and  $M_{\tilde{t}_R}$ . The mixing, however, further reduces the smaller of the two mass eigenstates [7]. (This effect is negligible for the first two generation squarks, because the corresponding quark mass entering eq. (2) is very small.) Since  $A_t$  is directly related to its boundary condition  $A_0$  at the GUT scale, one would expect that mSUGRA models with large values of  $|A_0|$  would have a light stop in their spectrum. As it turns out, a better parameter for light stop discussions is the dimensionless ratio  $a_0 \equiv A_0/\sqrt{M_0^2 + 4M_{1/2}^2} \simeq A_t/m_{\tilde{t}}$ , which can be easily understood from eqs. (1) and (2). Increasing either  $M_0$  or  $M_{1/2}$  would increase the diagonal entries in the stop mass matrix, and make the stop heavier, while  $A_0$  controls the size of  $A_t$  at the weak scale. In Fig. 1 we show contours of the lightest stop mass (in GeV) in the  $(a_0, \tan \beta)$  plane, for  $M_{1/2} = 300$  GeV,  $M_0 = 300$  GeV and  $\mu > 0$ . Inside the light-shaded region there is a scalar (stop, stau or CP-odd Higgs) which is too light or tachyonic. The dark-shaded region is theoretically allowed, but ruled out because of the CP-even Higgs mass limit of  $m_h > 95$  GeV. In calculating the light stop mass, we have included the full one-loop corrections to the stop mass matrix [8]. This is needed in order to reduce the scale dependence of  $m_{\tilde{t}_1}$ , which is known to be significant, especially in such cases of large stop mixing.

We see from Fig. 1 that a light stop is associated with a limited range of rather large values of  $|a_0|$ , where the stop mixing becomes very large. We have checked, by scanning the mSUGRA parameter space, that if  $\tan \beta \gtrsim 2.0$ , values of  $a_0$  between 0 and 2 would never lead to stop masses below 200 GeV.

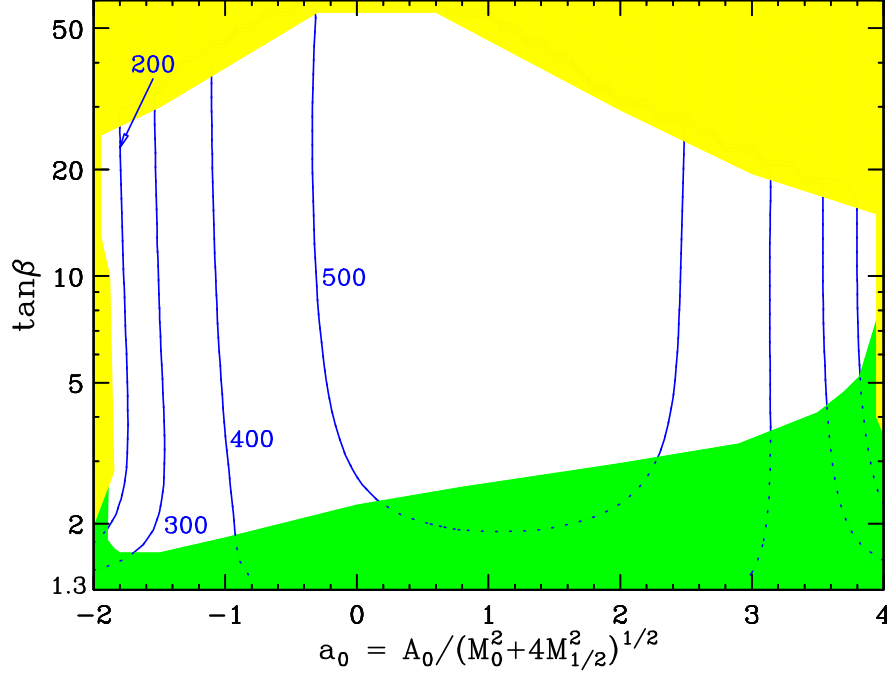


Figure 1: Contours of the light stop mass  $m_{\tilde{t}}$  (in GeV), versus the mixing parameter  $a_0$  and  $\tan\beta$ , for  $M_{1/2} = 300$  GeV,  $M_0 = 300$  GeV and  $\mu > 0$ . Inside the light-shaded region there is a scalar (stop, stau or CP-odd Higgs) which is too light or tachyonic. The dark-shaded region is theoretically allowed, but ruled out because of the CP-even Higgs mass limit of  $m_h > 95$  GeV.

Another possibility to have a light stop is that the soft mass parameters  $M_{\tilde{Q}_3}$  and  $M_{\tilde{t}_R}$  entering eq. (1) are small by themselves. This may be due to the RG evolution down from very high scales, which tends to order the squark soft masses in an inverse hierarchy with respect to their Yukawa couplings. Since the top Yukawa coupling  $\lambda_t$  is so large, the stops “feel” this RGE effect to a larger extent than the other squarks. As a result, the stop soft masses  $M_{\tilde{Q}_3}$  and  $M_{\tilde{t}_R}$  are typically smaller than the soft mass parameters of the other squarks. This effect is strongest when the top Yukawa coupling is the largest, i.e. at small values of  $\tan\beta$ . Indeed, Fig. 1 exhibits a region at rather small values of  $\tan\beta$ , where one may find a light stop for a very wide range of the  $A_0$  parameter. Very low values of  $\tan\beta$ , however, are excluded both experimentally and theoretically. In the MSSM, the lightest Higgs mass  $m_h$  is correlated with  $\tan\beta$  and current bounds on  $m_h$  from LEP all but exclude values of  $\tan\beta \lesssim 2.0$ . In Fig. 2 we show contours of the light Higgs mass  $m_h$ ,

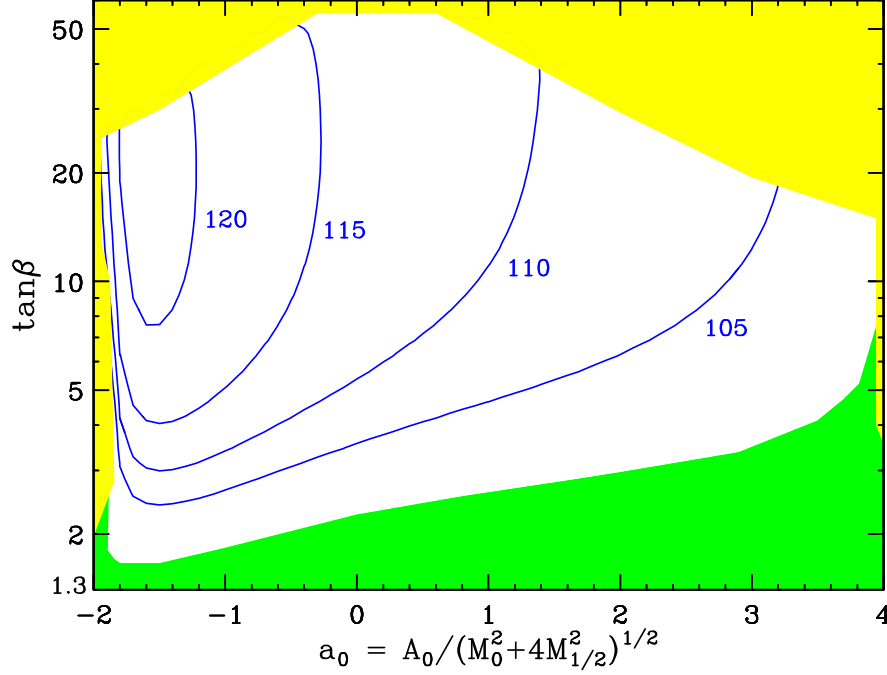


Figure 2: Contours of the light Higgs mass  $m_h$  (in GeV) for the same parameters as in Fig. 1.

for the same parameters as in Fig. 1. We see that the current Higgs bound already rules out the region where we get a light stop because of the large Yukawa RGE effects. This constraint may be relaxed in models with a non-minimal Higgs sector, like the NMSSM [9]. In that case, there is still a theoretical lower bound on  $\tan \beta \lesssim 1.3 - 1.5$ , which is due to the requirement that  $\lambda_t$  remains perturbative when extrapolated up to very high scales, e.g.  $M_P$ . What is more, from Fig. 2 we also see that the direct Higgs searches in Run II [10] also eat away from the light stop parameter space. If the Higgs escapes detection after the first stage of Run II ( $2 \text{ fb}^{-1}$  per detector), the expected  $m_h$  limit with (without) a neural network improvement of the analysis will be  $m_h > 120$  (105) GeV [10]. In that case, the mSUGRA light stop parameter space at  $a_0 > -1$  ( $a_0 > 3$ ) will also be ruled out. However, the light stop region at  $A_0 < 0$  may actually be more effectively probed via stop searches rather than via the Higgs search.

It is straightforward to check that the (very light) stop mass has no significant dependence on the other mSUGRA parameters. Our mSUGRA scan reveals that there exist

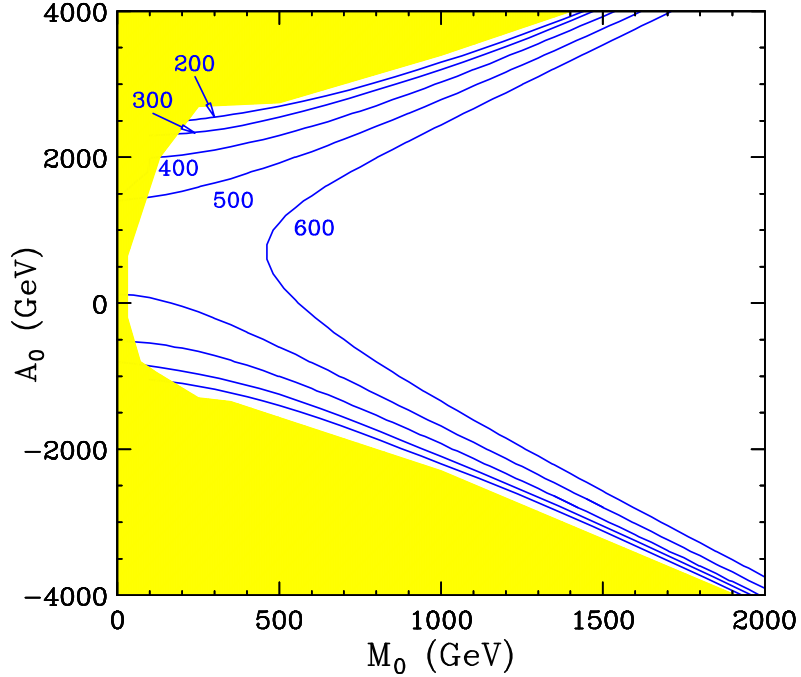


Figure 3: Contours of the light stop mass  $M_h$  (in GeV) in the  $M_0 - A_0$  plane, for fixed  $M_{1/2} = 300$  GeV,  $\tan\beta = 10$  and  $\mu > 0$ .

very light stop solutions for almost any values of  $M_0$  and  $M_{1/2}$ ! The reason is that there always exist large enough values of  $|A_0|$ , which can increase the amount of stop mixing and yield an arbitrarily light stop in the spectrum. This is illustrated in Fig. 3, where we show contours of the light stop mass in the  $M_0 - A_0$  plane, for fixed  $M_{1/2} = 300$  GeV,  $\tan\beta = 10$  and  $\mu > 0$ . This value of  $M_{1/2}$  is just beyond the Tevatron reach for chargino-neutralino searches in the trilepton channel [11]. We then see that for arbitrarily large  $M_0$ , i.e. heavy scalars, there is still a (rather limited) range of  $A_0$ , where of all SUSY searches in Run II, only the light stop searches have a chance of being successful. Of course, the branching ratios of the stop decays do depend on both  $M_0$  and  $M_{1/2}$ , and this will determine the degree of applicability of each of the channels that we are considering below. We shall comment on the relevant range for  $M_0$  and  $M_{1/2}$  in each case as we go along. Also notice that the production cross section for stops is almost independent of any of the MSSM parameters, and is uniquely determined by the stop mass.

We should point out that all stop search analyses below are pretty much model in-



dependent and have only a few mild assumptions about the sparticle spectrum. The motivation for having a light stop in the spectrum, on the other hand, is very model-dependent. For example, in mSUGRA very large values of  $|a_0|$  violate the naturalness criterion [12], implying that the odds for a light stop in mSUGRA are rather small. But the odds for mSUGRA being the correct model of SUSY breaking are probably pretty small too. So we adopt the stance that we should leave any theoretical prejudice behind and look for the stop in every conceivable channel, until the first experimental SUSY data are in.

## 2.2 Experimental assumptions

To determine the mass reach for various search modes in Run II we compare the number of expected signal events to a variation of the number of background events (assumed to be purely poissonian). A mass region is excluded if the signal is larger than 3 standard deviations of the background.

The number of events is calculated as a product of the integrated luminosity, production cross section and efficiency after final cuts.

The integrated luminosities of  $2 \text{ fb}^{-1}$ ,  $4 \text{ fb}^{-1}$  and  $20 \text{ fb}^{-1}$  were used as expectations for different stages of Run II.

At the Tevatron, third generation scalar quarks are expected to be produced in pairs via gluon-gluon fusion and quark-antiquark annihilation, and, consequently, the leading-order production cross section depends only on their masses. The next-to-leading order corrections increase the cross section and introduce a weak dependence on other masses and parameters ( $\sim 1\%$ ) [13]. Signal events were modeled using the PYTHIA generator [14].

In the following we assume that the increase in the production cross section due to variation of the center-of-mass energy from 1.8 to 2.0 TeV will be approximately 40% for the squark pair production. Background cross sections were also scaled with factors determined from the corresponding Monte Carlo generators [15] (20% for the  $W/Z$  production and QCD).

Our Run II efficiency estimates are based on the performance of the CDF detector in

Run I using the full detector simulation. When possible we extrapolated the results of existing CDF searches in corresponding channels.

CDF is a general purpose detector described in detail elsewhere [16]. The innermost part of CDF, a silicon vertex detector (SVX), allows a precise measurement of a track's impact parameter with respect to the primary vertex in the plane transverse to the beam direction. The momenta of the charged particles are measured in the central drift chamber which is located inside a 1.4 Tesla solenoidal magnet. Outside the drift chamber there is a calorimeter, which is organized into electromagnetic and hadronic components, with projective towers covering the pseudo-rapidity range  $|\eta| < 4.2$ . The muon system is located outside the calorimeter and covers the range in  $|\eta| < 1$ .

Jet energies are calculated using the calorimeter energy deposition within a cone in  $\eta - \phi$  space, where  $\phi$  is the angle in the plane normal to the beam direction. The missing transverse energy is defined as the energy imbalance in the directions transverse to the beam direction using the energy deposited in calorimeter towers with  $|\eta| < 3.7$ . A lepton is identified by either hits in a muon chamber or a cluster of energy in the electromagnetic calorimeter, and an associated track in the central tracking chamber.

Two heavy flavor tagging algorithms use the SVX information to tag charm and bottom quark jets, or c-jets and b-jets. In the Jet Probability (JP) algorithm the probability that the track comes from the primary vertex is determined taking into account the impact parameter resolution. This probability is smaller for heavy flavor decay products because of their considerable lifetime. The track probabilities for tracks associated to a jet are combined into JP [17]. We associate tracks to a jet by requiring that the track is within a cone of 0.4 in  $\eta - \phi$  space around the jet axis. Distribution of JP is flat by construction for light quark jets, originating from the primary vertex, and peaks at zero for heavy quarks. Since the JP is a continuous variable, the tagging can be optimized both for charm and bottom jets. In another heavy flavor tagging algorithm, SECVTX, a jet is identified as a bottom quark candidate if its decay point is displaced from the primary vertex [18]. This algorithm is not very efficient for the charm tagging.

In calculating Run II efficiencies we scaled by a factor of two the Run I efficiency for heavy flavor tagging. This factor accounts for the increase in the SVX geometrical acceptance due to the larger SVX length. Conservatively, we did not assume any other

improvements in the detector performance such as, for example, a better coverage for the lepton identification. The description of the upgraded CDF-II detector can be found in [19].

### 2.3 Reach in the $bj\ell\cancel{E}_T$ channel

If the chargino (either gaugino-like or higgsino-like) is lighter than the light stop, the dominant decay of the stop is  $\tilde{t} \rightarrow b\tilde{\chi}_1^+$  [20, 21, 22, 23, 24]. If there are no sfermions (squarks or sleptons) lighter than the chargino, the latter decays to a real or virtual  $W$  and the lightest neutralino. In this case stop decays produce top-like signatures:  $2W$ 's and 2 b-jets. The only differences are kinematical : higher  $\cancel{E}_T$  due to the massive neutralinos, different jet spectra and angular distributions.

There are two possible search strategies for this decay mode based on different signatures :  $b\ell j\cancel{E}_T$  and  $\ell^+\ell^-j\cancel{E}_T$ . We note that in the case of the dilepton signature one pays a price of the low lepton branching ratio twice. Here we present a sensitivity study based on the  $b\ell j\cancel{E}_T$  signature. We select events with an isolated electron or muon with  $p_T > 10$  GeV/c passing lepton identification cuts, and at least two jets, one with  $E_T > 12$  GeV and the second with  $E_T > 8$  GeV. At least one of the jets is b-tagged with the SECVTX algorithm. To decrease Drell-Yan and  $Z^0$  background we removed events with two isolated, opposite sign leptons. For the reduction of QCD background we also required  $\cancel{E}_T > 25$  GeV and  $\Delta\phi(\cancel{E}_T - \text{nearest jet}) > 0.5$ .

The main remaining backgrounds for this search are from the  $W + \text{jets}$  and top production. Table 1 lists the relative contributions of different backgrounds after all cuts for this channel together with two other experimental stop signatures to be considered later. In the table we quote the  $W(\rightarrow \tau\nu)+\text{jets}$  contribution separately because of possible hadronic decays of  $\tau$  which mimic a jet. The last line shows the total background cross section after final cuts.

Typical values of efficiencies after final cuts for this and other (considered below) stop signatures are shown in Fig. 4. The efficiencies are plotted as a function of the mass difference between the stop and its supersymmetric decay product. The mass difference effectively determines the kinematical properties of the reaction and, therefore, the ef-

Background process	Stop signature		
	$b\ell\ j\cancel{E}_T$	$cc\cancel{E}_T$	$\ell^+\ell^-j\cancel{E}_T$
$W(\rightarrow e(\mu)\nu)+\text{jets}$	52%	1%	-
$W(\rightarrow \tau\nu)+\text{jets}$	3%	52%	-
Drell-Yan, $Z+\text{jets}$	2%	8%	26%
$WW/WZ/ZZ$	-	3%	13%
$t\bar{t}$	21%	5%	21%
QCD (includes $b\bar{b}$ )	20%	23%	41%
Total cross section, fb	980	160	50

Table 1: Relative contribution of various backgrounds for the stop searches after final cuts and the total background cross sections.

ficiency. Straight line fits show the efficiency parametrizations used for our estimates.

We show the reach of Run II in this channel in Figure 5. Even with  $2\text{ fb}^{-1}$  of data we will be sensitive to stop masses up to  $m_t$ . The sensitivity vanishes when we approach the kinematic limit for this channel, because the b-jets become too soft. We see also that the projected reach for  $2\text{ fb}^{-1}$  completely overlaps with the region of expected sensitivity for chargino searches at LEP, but with higher luminosity the Tevatron will be able to extend those bounds.

Note that the leptonic branching ratio of the chargino can be significantly increased, if the (left-handed) sleptons are relatively light, which happens when  $M_0 \lesssim M_{1/2}$ . This would lead to a much larger Tevatron reach in this channel [25]. In the mSUGRA model we find that for  $M_0 \leq 0.55M_{1/2}$  the electron and muon sneutrinos are lighter than the chargino, which would increase the chargino branching ratio to leptons to almost 100%. In this case the dilepton signature, discussed in detail in 2.5, may give a better sensitivity.

When the sneutrinos are light, the leptonic branching ratios of gauginos are high and this region of parameter space can also be effectively probed via searches for chargino/neutralino production in the clean trilepton channel [11].

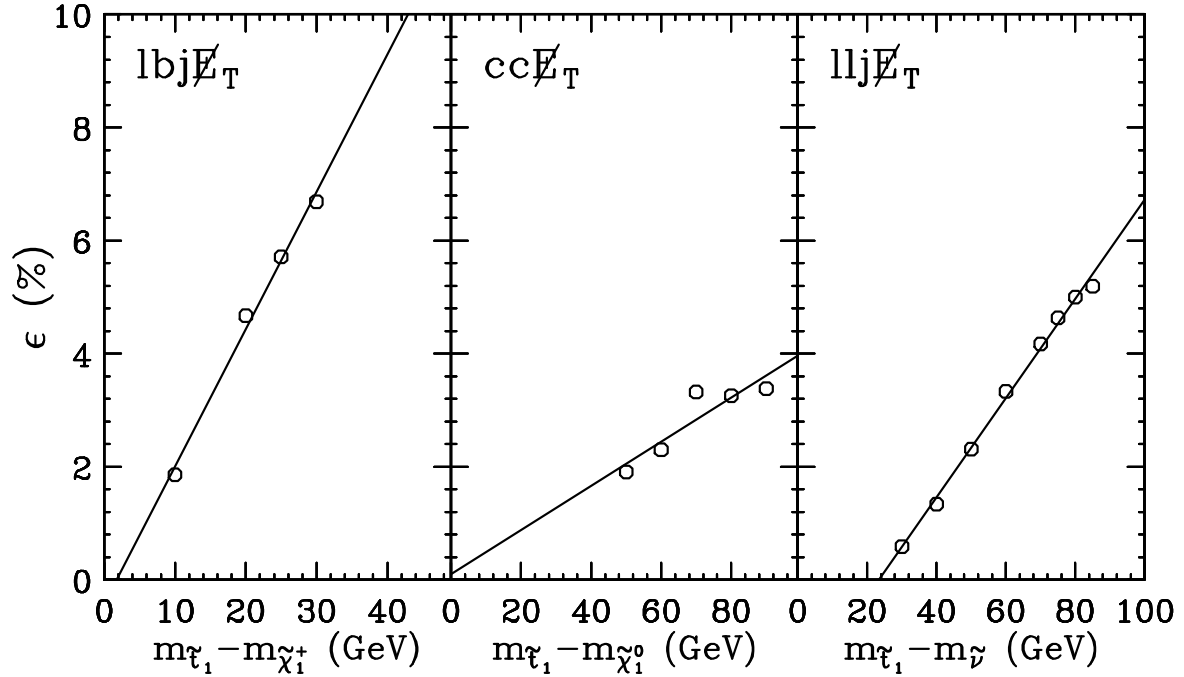


Figure 4: Typical values of efficiencies after final cuts for the stop signatures considered in the text.

A possible improvement in the analysis would be a requirement of an additional b-jet, given a much higher integrated luminosity in Run II. This cannot be afforded for Run I analyses because the signal efficiency becomes too low despite the formally better sensitivity.

## 2.4 Reach in the $cc\cancel{E}_T$ channel

This is the simplest, and in some sense, most model-independent situation, which arises whenever the stop is the next-to-lightest supersymmetric particle. Then, the only two-body stop decay still open is  $\tilde{t} \rightarrow c\tilde{\chi}_1^0$  [20, 22, 23]. In the absence of any flavor-changing effects in the squark sector (which is rather unlikely), this decay proceeds through a loop, otherwise it occurs at tree-level through stop-scharm mixing. The stop signature in this channel is two acolinear charm jets and missing transverse energy carried away by neutralinos. The events for this analysis in Run I were collected using a trigger which required  $\cancel{E}_T > 35$  GeV. We select events with 2 or 3 jets with  $E_T > 15$  GeV and  $|\eta| < 2$ .

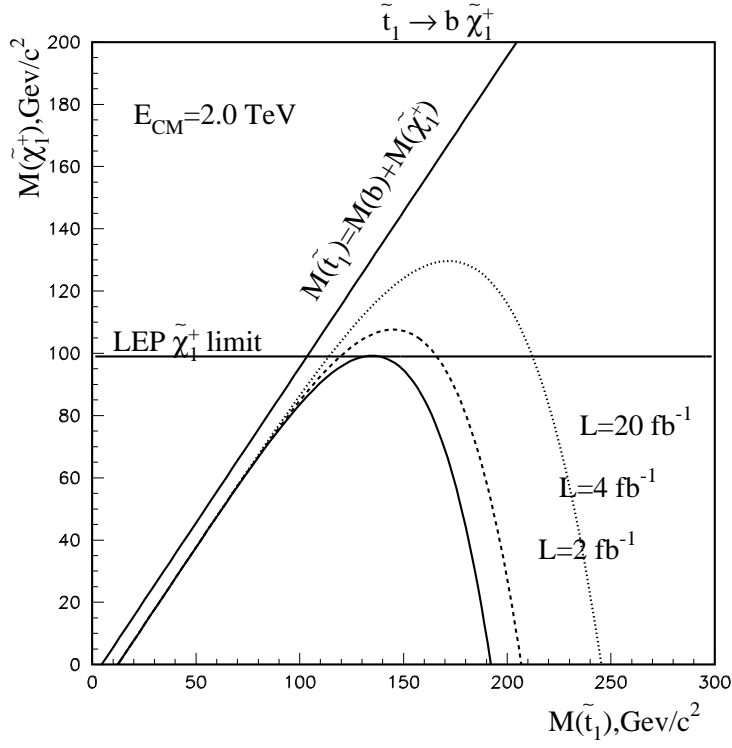


Figure 5: Sensitivity of the light stop search in the  $b\ell j \cancel{E}_T$  channel for several integrated luminosities. The analysis assumes 100% branching ratio for  $\tilde{t} \rightarrow b\tilde{\chi}_1^+$  and  $W$ -like branching ratios for the chargino decays.

The  $\cancel{E}_T$  cut is increased beyond the trigger threshold to 40 GeV and we require that the  $\cancel{E}_T$  is neither parallel nor anti-parallel to any of the jets in the event in order to reduce the contribution from the processes where the missing energy comes from jet energy mismeasurement:  $\min \Delta\varphi(\cancel{E}_T, j) > 45^\circ$ ,  $\Delta\varphi(\cancel{E}_T, j_1) < 165^\circ$ , and  $45^\circ < \Delta\varphi(j_1, j_2) < 165^\circ$ , where the jets are ordered in  $E_T$ . We also veto electrons and muons to suppress the  $W$ +jets background.

We use the JP algorithm to tag a charm jet requiring that at least one jet has a probability less than 0.05. This requirement, chosen to optimize the expected signal significance, rejects 97% of the background while its efficiency for the signal is 25%.

As can be seen from Table 1, the dominant source of remaining background for this analysis is  $W$ +jets production where the vector boson gives a hadronically decaying  $\tau$  lepton. There is also a contribution from QCD multijet production. The middle plot in Figure 4 shows the signal efficiency as a function of the stop and neutralino mass

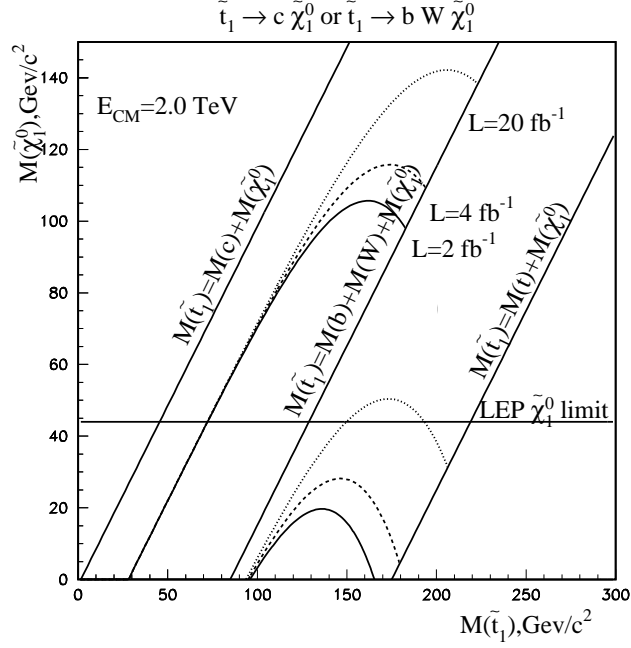


Figure 6: The same as Fig. 5, for the light stop search in the  $cc\cancel{E}_T$  and  $bj\ell\cancel{E}_T$  channels. The  $cc\cancel{E}_T$  ( $bj\ell\cancel{E}_T$ ) analysis assumes 100% branching ratio of  $\tilde{t} \rightarrow c\tilde{\chi}_1^0$  ( $\tilde{t} \rightarrow bW^+\tilde{\chi}_1^0$ ).

difference.

Figure 6 shows the Run II exclusion contours in this channel for several integrated luminosities. CDF Run Ib results for this channel were presented in [26]. The reach in stop mass is determined by the accumulated statistics while the reach in neutralino mass depends on the efficiency of our selection cuts, where the most limiting is the  $\cancel{E}_T$  cut, effectively fixed by the  $\cancel{E}_T$  trigger threshold. This is what determines the gap between the kinematic limit and the excluded region. In Run II CDF will have a possibility to use the secondary vertex information at the trigger level [27]. Addition of a displaced track requirement may allow to lower the  $\cancel{E}_T$  trigger threshold to 25 GeV and, therefore, significantly extend the excluded region to the kinematic limit. Even with the high  $\cancel{E}_T$  cut, we see that already with 2 fb<sup>-1</sup> the Tevatron will be able to probe regions well beyond the sensitivity of LEP searches.

If the mass gap between the stop and neutralino masses is larger than  $m_b + M_W$ ,

the three-body decay  $\tilde{t} \rightarrow bW^+\tilde{\chi}_1^0$  opens up. We use the signature  $b\ell j\cancel{E}_T$  discussed in Section 2.3 to estimate the sensitivity for this kinematic region (see Fig. 6).

## 2.5 Reach in the $jl^+l^-\cancel{E}_T$ channel

If the stop is lighter than the chargino, but heavier than any of the sleptons, then the three body decay modes  $\tilde{t} \rightarrow b\ell^+\tilde{\nu}_\ell$  and  $\tilde{t} \rightarrow b\tilde{\ell}^+\nu_\ell$  become dominant [20, 22, 28]. Such a situation may readily arise in the minimal SUGRA model. As we mentioned in Sec. 2.3, for  $M_0 \leq 0.55 \cdot M_{1/2}$ , the sneutrinos are lighter than the chargino. In those cases, there almost always exist values for  $A_0$  (both negative and positive) which will bring the light stop mass in between  $m_{\tilde{\nu}}$  and  $m_{\tilde{\chi}_1^+}$ .

Since in this case the stop leptonic branching ratio is high, we can afford to require two leptons in the final state. A  $b$ -tag is not required in order to save on jet acceptance. We select events with two leptons  $P_T(\ell_1) > 8$  GeV/c and  $P_T(\ell_2) > 5$  GeV/c,  $\cancel{E}_T > 30$  GeV and at least one jet with  $E_T > 15$  GeV. In order to suppress the  $b\bar{b}$  background, we require the leptons to be isolated – the calorimeter energy sum in a cone of 0.4 in  $\eta - \phi$  space around both leptons should be less than 5 GeV. Further cuts on the angle between either of the leptons and the missing transverse energy reduce the background from jet mismeasurement:  $\Delta\varphi(\ell, \cancel{E}_T) > 20^\circ$  and  $\Delta\varphi(\text{dilepton system}, \cancel{E}_T) > 20^\circ$ . The main backgrounds are Drell-Yan dilepton production, top,  $b\bar{b}$  and QCD multijet production (see Table 1). The right plot in Figure 4 shows the signal efficiency as a function of the stop and sneutrino mass difference. We show the reach of Run II in this channel in Figure 7. Again, we see that the Tevatron will be able to go well beyond the LEP limits.

At large values of  $\tan\beta$ , the same two effects that can lead to a light stop – the enhanced RGE renormalization and the larger mixing, can also make the lightest tau slepton significantly lighter than the electron or muon sneutrino/slepton. (Note that because of the large stau mixing, now the chargino can couple to the lightest stau, so we are not limited to considering only the sneutrinos, which are typically heavier.) Therefore, there are larger regions in the mSUGRA parameter space where one encounters the hierarchy  $m_{\tilde{\tau}} < m_{\tilde{\chi}_1^+}$  instead. In the minimal SUGRA model this is possible for  $M_0 \lesssim 5M_{1/2}$ . In that case, the three-body stop decay  $\tilde{t} \rightarrow b\tilde{\tau}_1^+\bar{\nu}_\tau$  may be dominant, giving rise to the



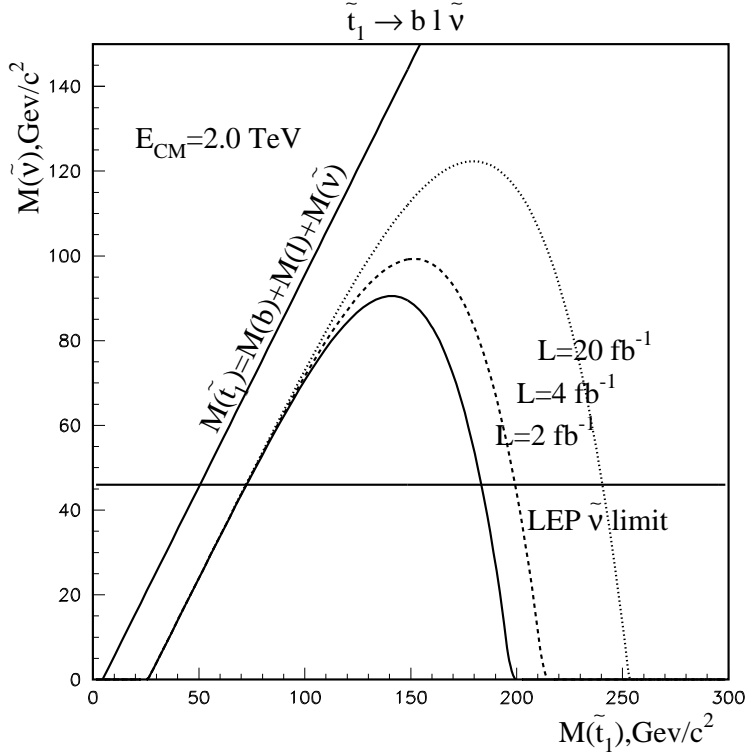


Figure 7: The same as Fig. 5, but for the light stop search in the  $b\ell^+\ell^-j\cancel{E}_T$  channel, assuming that the stop decays as  $\tilde{t} \rightarrow b\ell^+\tilde{\nu}_\ell$  and  $\tilde{t} \rightarrow b\ell^+\nu_\ell$ .

signature  $b\bar{b}\tau^+\tau^-\cancel{E}_T$ . Since the leptons from the tau decays are rather soft, it may be advantageous to consider a signature where we replace one of the leptons with an identified tau jet:  $b\ell\tau j\cancel{E}_T$  [29].

### 3 Higgsino LSP

So far we have been considering only minimal SUGRA models, which assume universality of the scalars and gauginos at the unification scale  $M_{\text{GUT}}$ . Theoretically, however, this assumption is not very well motivated. If gravitational interactions are the mediator of supersymmetry breaking, then universality would naturally hold at the Planck scale  $M_{\text{P}}$  instead, and may get modified by whatever physics there is between  $M_{\text{GUT}}$  and  $M_{\text{P}}$ . If there is grand unification, however, the GUT symmetry will preserve universality multiplet by multiplet. Thus one may expect that sparticles belonging to the same GUT representation still have identical soft masses at the GUT scale; while sparticles belonging to *different* GUT representations may have different soft masses. Within the framework

of a SUSY SU(5) GUT, this implies that the universal scalar mass parameter  $M_0$  is now being replaced by 4 scalar mass inputs at the GUT scale:  $M_{10}$ , the mass of the two up-type squarks, the left-handed down squark and the right-handed selectron;  $M_5$ , the mass of the right-handed down-type squark and the left-handed slepton doublet; and  $M_{H_1}$  ( $M_{H_2}$ ) — the soft mass for the down-type (up-type) Higgs doublet. This type of model has become known as the non-universal SUGRA model.

The non-universality in the boundary conditions for the scalar masses affects the SUSY mass spectrum in several ways. First, and most directly, it may change the ratios of various scalar masses, for example the left-handed and right-handed charged sleptons. However, the values of the scalar masses at low energies also depend on the gaugino masses through the RGE evolution, and the effects from any scalar mass non-universalities become diluted in the limit  $M_0 \ll M_{1/2}$ . A true test of universality will therefore require measuring several squark or slepton masses to a very good precision, something which may only be accomplished at the next linear collider.

There are also indirect implications of scalar mass non-universality. The higgsino mass parameter  $\mu$ , which is determined from the condition of electroweak symmetry breaking, is sensitive to the soft mass spectrum of the Higgses and third generation sfermions. In the minimal SUGRA model, it turns out that typically the higgsino masses are quite a bit larger than the gaugino ones, and as a result, the LSP and the lightest chargino are mostly gaugino-like<sup>1</sup>. In the non-universal SUGRA model, where the two Higgs soft masses are free inputs at the GUT scale, we often find regions of parameter space where  $|\mu| < M_1$ , and as a result, the two lightest neutralinos and the light chargino are almost degenerate and mostly higgsino-like. Relaxing the universality assumption for the gaugino masses may also lead to higgsino-like LSP [31].

The implicit assumption for all three stop searches in the previous Section was that the LSP is gaugino-like. In case of a higgsino-like LSP, the search strategy obviously needs to be modified.

The analysis in Sections 2.3 relies on the presence of a hard lepton from the chargino

---

<sup>1</sup> There is one possible exception to this rule – for multi-TeV  $M_0$  one can find natural [12] regions of  $|\mu| < M_1, M_2$  [30], where  $M_1$  and  $M_2$  are the SUSY breaking mass parameters for the  $U(1)_Y$  and  $SU(2)_L$  gauginos, respectively.

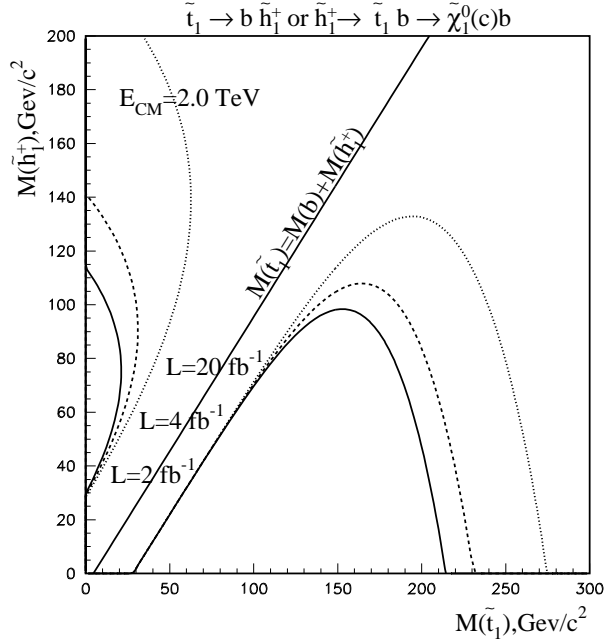


Figure 8: Sensitivity to  $\tilde{t} \rightarrow b\tilde{h}^+$  or  $\tilde{h}^+ \rightarrow \tilde{t}b$  decays for different integrated luminosities.

decay. If the chargino is higgsino-like, it is very close in mass with the LSP and the leptons from the chargino decays are too soft to be used for either triggering or off-line. The analysis in Section 2.5 assumes the existence of a significant mass gap between the LSP and the lightest chargino, bigger than the gap between the LSP and the stop itself. This is not true if the LSP is higgsino-like. In fact, the dominant stop decay in that case is  $\tilde{t} \rightarrow b\tilde{\chi}_1^+$ . The subsequent chargino decay to  $\tilde{\chi}_1^0$  is associated with very soft leptons or jets. The only observable signature therefore is  $b\bar{b}\cancel{E}_T$  [32]. It is similar to the signature considered in Section 2.4, except that now the heavy flavor jets are b-jets. To understand our sensitivity to stop in this channel we apply all the cuts discussed in Section 2.4. We gain some sensitivity with respect to the  $cc\cancel{E}_T$  analysis because the heavy flavor tagging technique that we use is more efficient to bottom than to charm.

A family of curves below the diagonal in Fig. 8 represent the reach of Run II in the  $b\bar{b}\cancel{E}_T$  channel for different integrated luminosities. We see that we restore our sensitivity to stop discovery even though the higgsino decay products are lost. The reach is similar

to the one presented in Fig. 6 for the  $c\cancel{E}_T$  channel.

## 4 Stop search in chargino (higgsino) production

It may be that the stop is light, yet cannot be found by regular means since it is almost degenerate with the LSP and its decay products are too soft to be observed. Such regions of the SUGRA parameter space readily exist, and under those rather unfortunate circumstances one should look for stops among the decay products of some other, rather light particles<sup>2</sup>. Let us review our options.

Of all the SM particles, the only ones likely to be heavier than the stop are the top and possibly the Higgs(es), but the production cross sections for the latter at the Tevatron are too small to be relevant. Top quarks may in principle decay to stops and gluinos [35]. This channel is usually closed, since the gluino is typically quite heavy. Some unconventional models [4] predict a light gluino in the tens of GeV range, with the gluino possibly being the LSP. However, existing data already rule out the range of gluino masses for which the two-body decay  $t \rightarrow \tilde{t}_1 \tilde{g}$  is open [4]. Top quarks may also decay to stops and neutralinos [22, 36]. One can look for these decays through precise measurements of the top branching ratios. If the stop is really degenerate with the LSP, it decays invisibly, and as a result the signature is an invisible top. If the  $\tilde{t} - \tilde{\chi}_1^0$  mass difference is large enough so that the  $c$ -jets can be detected, yet small enough to evade the stop search in the  $c\cancel{E}_T$  channel, then the signature will be top quarks decaying to  $t \rightarrow c\cancel{E}_T$ . The top cross section is big, but the width into  $Wb$  is also quite large, so these will be quite challenging analyses.

We now turn to discuss the possibility of producing stops in SUSY cascades. Among the remaining SUSY particles, gluinos have the largest production cross section, and they can decay to  $t\bar{t}$  pairs [21, 22, 37]. Since the stops are invisible, the signature is similar to the leptonic channels of top pair production. The crucial difference from  $t\bar{t}$  production is that because of the Majorana nature of the gluino, half of the time the top quarks will have the same sign. Such an analysis is also in preparation for Run II.

One can also consider neutralino decays to top-stop. In this case, however, the neu-

---

<sup>2</sup>In the case of an extreme degeneracy with the LSP (which is somewhat preferred on the basis of relic density arguments [33]), the stops can be long lived and form bound states, “top squarkonia” [34], which eventually decay through  $\tilde{t}_1 \tilde{t}_1^*$  annihilation.

tralininos would have to be heavier than  $m_t + m_{\tilde{t}}$ . Since their cross sections are electroweak, they would be too small to be observed at the Tevatron.

Stops may also appear in sbottom decays:  $\tilde{b} \rightarrow \tilde{t}W^-$  or  $\tilde{b} \rightarrow \tilde{t}H^-$ , but first, these processes will have to compete with  $\tilde{b} \rightarrow b\tilde{\chi}_1^0$ , which is preferred by phase space, and second, since stops are invisible, the final state signatures ( $W^+W^-$ ,  $W^+H^-$  or  $H^+H^-$ ) will have very large backgrounds.

Finally, we can consider production of charginos, which later decay to stops:  $\tilde{\chi}^+ \rightarrow \tilde{t}\bar{b}$  [32]. This case looks more promising than the neutralino decays to stops. First, there is much less phase space suppression, and second, for gauginos, the chargino pair production cross sections are larger than the neutralino ones. In the rest of this Section we shall consider this channel in more detail.

We start by assuming that the LSP is mostly Bino. (If it were higgsino, we are back to the case discussed in Section 3). Then, if the SUGRA relations among the gaugino masses hold, the gaugino-like chargino would have to be twice as heavy. We shall consider  $\mu$  as a free parameter, which can be easily accounted for by non-universalities as discussed previously. Then, if  $|\mu| \ll M_2$ , the lighter chargino will be higgsino-like; while if  $|\mu| \gg M_2$ , we are back to the typical mSUGRA case of gaugino-like chargino.

Since the stop is almost degenerate with the neutralino by our assumption in this section, the resultant charm jets from its decay are very soft and cannot be detected, so the final state signature will be  $b\bar{b}\cancel{E}_T$  and we can consider the same selection which was used in Section 2.4. Yet the production cross section is different, since in this case we need to produce charginos via a weak process. In Fig. 9 we show a plot of the signal cross section times branching ratio versus the lightest chargino mass  $m_{\tilde{\chi}_1^+}$ . The mass, as well as the gaugino/higgsino mixture of the lightest chargino in the figure are varied by changing  $\mu$ , simultaneously adjusting  $A_t$  so that to keep the lightest stop degenerate with the LSP. The rest of the sparticle spectrum is assumed to be very heavy. We have also included the contributions from relevant processes with heavier neutralinos which may decay to  $\tilde{\chi}_1$ . We use conservatively leading order results for chargino/neutralino production; next-to-leading order QCD corrections can increase the signal by 20-30% [38]. We see from Fig. 9 that the signal cross section is rather small, and for the range of chargino masses beyond the LEP coverage, the signal is only a few hundred fb.

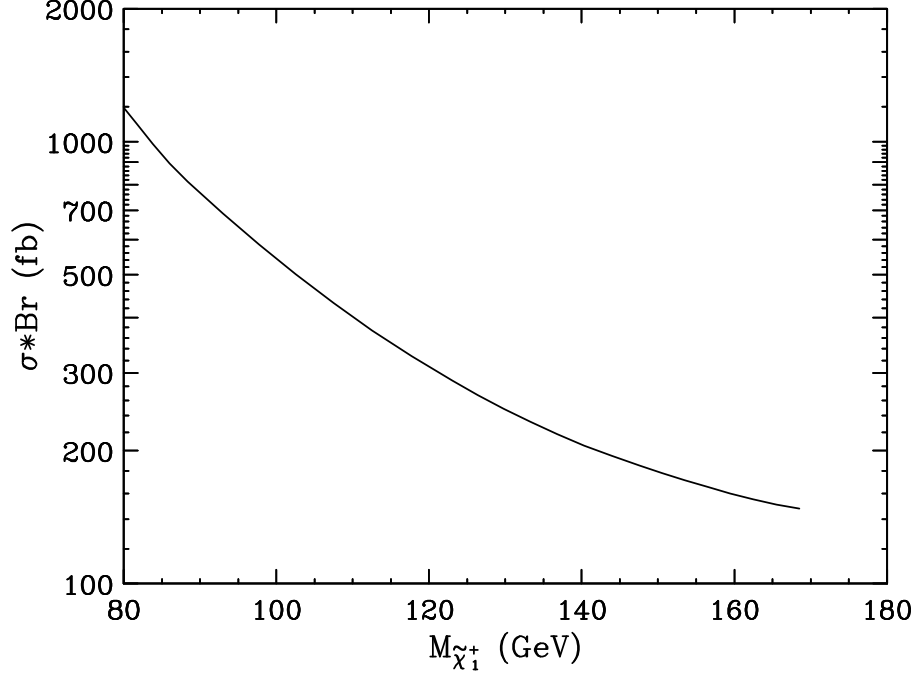


Figure 9:  $\sigma * \text{Br} \equiv \sum_{i,j} \sigma(\tilde{\chi}_i^+ \tilde{\chi}_j^-) \text{Br}(\tilde{\chi}_i^+ \rightarrow \tilde{t}_1 \bar{b}) \text{Br}(\tilde{\chi}_j^- \rightarrow \tilde{t}_1^* b)$  as a function of the chargino mass  $m_{\tilde{\chi}_1^+}$ , which is varied by changing  $\mu$ . We fix  $M_2 \sim 2M_1 = 180$  GeV, and appropriately adjust  $A_t$  so that the lightest stop is degenerate with the LSP. The rest of the sparticle spectrum is taken to be very heavy.

Our reach of Run II in this channel is presented by a family of curves above the diagonal in Fig. 8. Again, we can recover some region in parameter space by using an alternative signature in our search, but the absolute reach is not very impressive, mostly because of the small production cross sections.

## 5 Light bottom squarks

Light sbottoms in the mSUGRA model can appear only at small  $M_{1/2}$  and small  $M_0$ . In addition, they are always accompanied by light stops as well. In fact, throughout the whole mSUGRA parameter space,  $m_{\tilde{b}_1} > m_{\tilde{t}_1}$ . The only exception appears at values of  $\tan\beta > 20$  and  $\mu < 0$ , where we find that  $-60 \text{ GeV} < m_{\tilde{b}_1} - m_{\tilde{t}_1} < 0$ . (The correlation with the sign of  $\mu$  is due to the SUSY threshold corrections to the bottom Yukawa coupling [39].) However, this part of parameter space is severely constrained [40] by the  $b \rightarrow s\gamma$

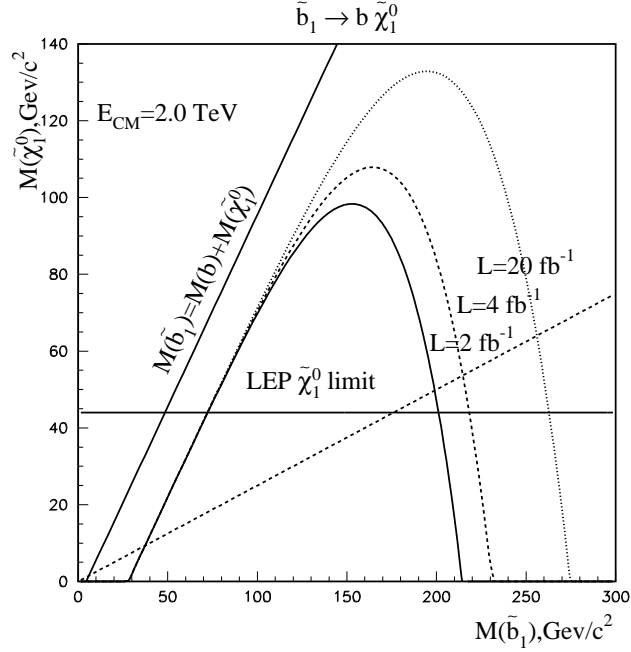


Figure 10: Sensitivity of the light sbottom search in the bottom neutralino channel for different integrated luminosities.

measurement from LEP [41]. Similar conclusions hold even when we relax scalar mass universality.

In any case, having done the analysis for stops decaying to higgsinos, it is straightforward to extend it to the case of sbottom production and sbottoms decaying directly to LSP's. Again we can consider the same selection used in Section 2.4 to estimate our sensitivity to a direct sbottom search. Our reach in Run II is presented in Fig. 10. Although the cross section of sbottom production is roughly equal to the stop production cross section for the same squark mass, our reach in sbottom mass is somewhat higher than in stop mass in the similar  $c\bar{c}\cancel{E}_T$  channel – compare to Fig. 6. This is due to the higher bottom tagging efficiency as compared to charm tagging efficiency.

By scanning the mSUGRA parameter space, we found that the universality assumption leads to the relation  $m_{\tilde{\chi}_1^0} \leq 0.25 m_{\tilde{b}_1}$  so that the mSUGRA parameter space maps onto the region below the dotted line in Fig. 10. Relaxing scalar mass universality, we still find that typically  $m_{\tilde{\chi}_1^0}/m_{\tilde{b}_1} \lesssim 0.25$ , but this ratio may go up to 0.4 for  $\tan\beta > 20$  and

$\mu < 0$ , which is in conflict with  $b \rightarrow s\gamma$ . This means that the observation of a signal in this channel already in Run II, if interpreted as sbottom production, will hint towards a more unconventional low-energy SUSY, for example non-universal gaugino masses.

## 6 Stop (sbottom) as NLSP in gauge-mediated models

Gauge mediation is an intriguing alternative for communicating supersymmetry breaking to the visible sector (MSSM) [42]. It offers the potential of solving the supersymmetric flavor problem, and leads to novel collider phenomenology [43].

The minimal gauge-mediated models, where the only SUSY breaking contributions to the scalar masses are from SM gauge loops, do not predict a light stop in the spectrum. However, one can easily imagine non-minimal extensions with extra gauge groups [44] or more complicated messenger sectors [45], which may lead to a light stop. Gauge mediated models are characterized by a Goldstino LSP  $\tilde{G}$ , which is almost massless. Of course, all our previous results hold for the case of gauge mediated models with a stable neutralino NLSP, since in that case the phenomenology is no different from SUGRA models. But what is more, our results from Sections 2.4 and Section 5 may be applied for the case of stop and sbottom NLSP, which decays promptly to the Goldstino. Identifying the neutralino LSP with the Goldstino, and taking the limit  $m_{\tilde{\chi}_1^0} \rightarrow 0$ , we can read off the Run II stop (sbottom) mass reach from the  $x$ -axis in Fig. 6 (Fig. 10). For example, if the dominant prompt decay of the stop is the three-body mode  $\tilde{t}_1 \rightarrow bW^+\tilde{G}$  [46], we can see that already with  $2 \text{ fb}^{-1}$  the Tevatron will be sensitive to light stop masses up to 160 GeV.

Prompt stop decays in gauge-mediated models can be expected only if the SUSY breaking scale is very low. Otherwise, the stops first hadronize in supersymmetric sbaryon or mesino states and then decay over macroscopic distances, leading to events with highly-ionizing tracks or displaced jets and large  $\cancel{E}_T$  [47]. It was recently pointed out, that in the case of prompt decays, stop mesino-antimesino oscillations can provide a very distinctive signature of like-sign top quark events [47].



## 7 Conclusions

There are various ways to look for a light stop, depending on the rest of the sparticle spectrum. We presented a long list of stop signatures which can be looked for in Run II of the Tevatron with upgraded detectors. There are also numerous other possible stop signals. For example, models with broken R-parity allow for a set of stop decays beyond the ones considered here [48], as well as associated (single) stop production processes [49]. Also, the 4-body decay of the stop can become dominant in certain models with suppressed flavor-changing effects [50].

In most cases the upcoming Tevatron runs can extend the LEP-II reach [51].

*Acknowledgements:* We would like to thank M. Carena and M. Peskin for discussions. Fermilab is operated by URA under DOE contract DE-AC02-76CH03000.

## References

- [1] W. de Boer, A. Dabelstein, W. Hollik, W. Möhle and U. Schwickerath, Zeit. Phys. **C75**, 627 (1997), [hep-ph/9607286](#); W. de Boer, R. Ehret, J. Lautenbacher, A. Gladyshev and D. Kazakov, preprint IEKP-KA-97-15, [hep-ph/9712376](#); P. Chankowski, talk given at the International Workshop on Quantum Effects in the MSSM, Barcelona, September 1997, [hep-ph/9711470](#); J. Erler and D.M. Pierce, Nucl. Phys. **B526**, 53 (1998), [hep-ph/9801238](#); D.M. Pierce, talk presented at the DPF Conference, Los Angeles, CA, January 5-9, 1999, <http://www.physics.ucla.edu/dpf99/trans/1-24.pdf>.
- [2] M. Carena, M. Quiros and C.E. Wagner, Phys. Lett. **B380**, 81 (1996), [hep-ph/9603420](#); Nucl. Phys. **B503**, 387 (1997), [hep-ph/9702409](#); Nucl. Phys. **B524**, 3 (1998), [hep-ph/9710401](#); D. Delepine, J.M. Gerard, R. Gonzalez Felipe and J. Weyers, Phys. Lett. **B386**, 183 (1996), [hep-ph/9604440](#); J. McDonald, Phys. Lett. **B413**, 30 (1997), [hep-ph/9707290](#); J.M. Cline and G.D. Moore, Phys. Rev. Lett. **81**, 3315 (1998), [hep-ph/9806354](#).
- [3] G. Farrar, Phys. Rev. **D51**, 3904 (1995), [hep-ph/9407401](#); Phys. Rev. Lett. **76**, 4111 (1996), [hep-ph/9603271](#); Nucl. Phys. Proc. Suppl. **62**, 485 (1998), [hep-ph/9710277](#).
- [4] S. Raby, Phys. Lett. **B422**, 158 (1998), [hep-ph/9712254](#) ; S. Raby and K. Tobe, Nucl. Phys. **B539**, 3 (1999), [hep-ph/9807281](#); H. Baer, K. Cheung and J. F. Gunion, Phys. Rev. **D59**, 075002 (1999), [hep-ph/9806361](#).
- [5] J. Feng and T. Moroi, Phys. Rev. **D58**, 5001 (1998), [hep-ph/9712499](#).
- [6] B. Allanach *et al.*, Contributed to “Physics at Run II: Workshop on Supersymmetry and Higgs”, Summary Meeting, Batavia, IL, 19-21 Nov. 1998, [hep-ph/9906224](#); H. Dreiner, in “Perspectives on supersymmetry”, ed. by G. L. Kane, [hep-ph/9707435](#).
- [7] J. Ellis and S. Rudaz, Phys. Lett. **B128**, 248 (1983).
- [8] D. Pierce, J. Bagger, K. Matchev and R.-J. Zhang, Nucl. Phys. **B491**, 3 (1997), [hep-ph/9606211](#).

- [9] See, e.g., U. Ellwanger and C. Hugonie, preprint LPT-ORSAY-99-65, **hep-ph/9909260**, and references therein.
- [10] Final Report of the Higgs Working Group, <http://fnth37.fnal.gov/higgs/draft.html>.
- [11] K. Matchev and D. Pierce, preprint FERMILAB-PUB-99/078-T, **hep-ph/9904282**; preprint FERMILAB-PUB-99/209-T, **hep-ph/9907505**; H. Baer, M. Drees, F. Paige, P. Quintana and X. Tata, preprint FSU-HEP-990509, **hep-ph/9906233**; V. Barger and C. Kao, **hep-ph/9811489**, v. 3 and 4.
- [12] J. L. Feng, K. T. Matchev and T. Moroi, preprint IASSNS-HEP-99-78, **hep-ph/9908309**; preprint IASSNS-HEP-99-81, **hep-ph/9909334**.
- [13] W. Beenakker *et al.*, Nucl. Phys. **B515**, 3 (1998).
- [14] T. Sjöstrand, Comp. Phys. Comm. **82**, 74 (1994), S. Mrenna, Comp. Phys. Comm. **101**, 232 (1997).
- [15] F. A. Berends, H. Kuijf, B. Tausk and W. T. Giele, Nucl. Phys. **B357**, 32 (1991); W. T. Giele, E. W. Glover and D. A. Kosower, Nucl. Phys. **B403**, 633 (1993), **hep-ph/9302225**.
- [16] F. Abe *et al.*, Nucl. Instrum. Methods **A271**, 387 (1988); P. Azzi *et al.*, Nucl. Instrum. Methods **A360**, 137 (1995).
- [17] F. Abe *et al.*, Phys. Rev. **D53**, 1051 (1996).
- [18] F. Abe *et al.*, Phys. Rev. Lett. **74**, 2626 (1995).
- [19] “The CDF II Detector”, Technical Design Report, preprint FERMILAB-Pub-96/390-E.
- [20] K. Hikasa and M. Kobayashi, Phys. Rev. **D36**, 724 (1987).
- [21] A. Bartl, W. Majerotto, B. Mossbacher, N. Oshimo and S. Stippel, Phys. Rev. **D43**, 2214 (1991).

- [22] H. Baer, M. Drees, R. Godbole, J.F. Gunion and X. Tata, Phys. Rev. **D44**, 725 (1991).
- [23] H. Baer, J. Sender and X. Tata, Phys. Rev. **D50**, 4517 (1994), [hep-ph/9404342](#).
- [24] J. L. Lopez, D. V. Nanopoulos and A. Zichichi, Mod. Phys. Lett. **A10**, 2289 (1995), [hep-ph/9406254](#); J. Sender, Phys. Rev. **D54**, 3271 (1996).
- [25] A. Datta, M. Guchait and K. K. Jeong, Int. J. Mod. Phys. **A14**, 2239 (1999), [hep-ph/9903214](#).
- [26] Chris Holck (for the CDF collaboration), “Search for Scalar Top”, Contributed Paper to the 29th International Conference on High-Energy Physics (ICHEP 98), Vancouver, British Columbia, Canada, July 23-30, 1998; preprint FERMILAB-CONF-98/208-E.
- [27] S. Donati, “The CDF Silicon Vertex Tracker”, Proceedings of the ”VI Advanced Computing Conference in Physics Research”, University of Crete, April 12-16, 1999.
- [28] W. Porod and T. Wohrmann, Phys. Rev. **D55**, 2907 (1997), [hep-ph/9608472](#); W. Porod, Phys. Rev. **D59**, 095009 (1999), [hep-ph/9812230](#).
- [29] H. Baer, C.-H. Chen, M. Drees, F. Paige and X. Tata, Phys. Rev. Lett. **79**, 986 (1997), [hep-ph/9704457](#); Phys. Rev. **D58**, 075008 (1998), [hep-ph/9802441](#); J. Lykken and K. Matchev, preprint FERMILAB-PUB-99/034-T, [hep-ph/9903238](#); preprint FERMILAB-Conf-99-270-T.
- [30] K. L. Chan, U. Chattopadhyay, and P. Nath, Phys. Rev. **D58**, 096004 (1998), [hep-ph/9710473](#).
- [31] G. Anderson, H. Baer, C.-H. Chen and X. Tata, preprint FSU-HEP-981015, [hep-ph/9903370](#).
- [32] K. Matchev, talk given at the SUSY’98 conference, July 11-17 1998, Oxford, England, <http://hepnts1.rl.ac.uk/SUSY98>.

- [33] M. Fukugita, H. Murayama, M. Yamaguchi and T. Yanagida, Phys. Rev. Lett. **72**, 3009 (1994); K. A. Olive and S. Rudaz, Phys. Lett. **B340**, 74 (1994), hep-ph/9408280.
- [34] M.J. Herrero, A. Mendez and T.G. Rizzo, Phys. Lett. **B200**, 205 (1988); V. Barger and W.Y. Keung, Phys. Lett. **B211**, 355 (1988); H. Inazawa and T. Morii, Phys. Rev. Lett. **70**, 2992 (1993); M. Drees and M.M. Nojiri, Phys. Rev. **D49**, 4595 (1994), hep-ph/9312213.
- [35] See, e.g., S. H. Zhu and L. Y. Shan, hep-ph/9811430.
- [36] S. Mrenna and C.P. Yuan, Phys. Lett. **B367**, 188 (1996), hep-ph/9509424; A. Brignole, F. Feruglio and F. Zwirner, Z. Phys. **C71**, 679 (1996), hep-ph/9601293; M. Drees, R.M. Godbole, M. Guchait, S. Raychaudhuri and D.P. Roy, Phys. Rev. **D54**, 5598 (1996) , hep-ph/9605447; C.S. Li, R.J. Oakes and J.M. Yang, Phys. Rev. **D54**, 6883 (1996), hep-ph/9606385; G. Mahlon and G.L. Kane, Phys. Rev. **D55**, 2779 (1997), hep-ph/9609210; M. Hosch, R.J. Oakes, K. Whisnant, J.M. Yang, B. Young and X. Zhang, Phys. Rev. **D58**, 034002 (1998), hep-ph/9711234.
- [37] G.L. Kane and S. Mrenna, Phys. Rev. Lett. **77**, 3502 (1996) , hep-ph/9605351.
- [38] W. Beenakker, M. Klasen, M. Krämer, T. Plehn, M. Spira and P. M. Zerwas, preprint CERN-TH/99-159, hep-ph/9906298.
- [39] L. J. Hall, R. Rattazzi and U. Sarid, Phys. Rev. **D50**, 7048 (1994), hep-ph/9306309; M. Carena, M. Olechowski, S. Pokorski and C. E. Wagner, Nucl. Phys. **B426**, 269 (1994), hep-ph/9402253; R. Hempfling, Zeit. Phys. **C63**, 309 (1994), hep-ph/9404226; M. Carena and C. E. Wagner, preprint CERN-TH-7321-94, hep-ph/9407209.
- [40] H. Baer and M. Brhlik, Phys. Rev. **D55**, 3201 (1997), hep-ph/9610224; J.L. Hewett and J.D. Wells, Phys. Rev. **D55**, 5549 (1997), hep-ph/9610323; T. Blazek and S. Raby, Phys. Rev. **D59**, 095002 (1999), hep-ph/9712257; H. Baer, M. Brhlik, D. Castano and X. Tata, Phys. Rev. **D58**, 015007 (1998), hep-ph/9712305; K. T. Matchev and D. M. Pierce, Phys. Lett. **B445**, 331 (1999), hep-ph/9805275.

- [41] F. Palla, [hep-ex/9905017](#); R. Barate *et al.* [ALEPH Collaboration], Phys. Lett. **B429**, 169 (1998); G. Eigen, [hep-ex/9901005](#).
- [42] See, e.g. G. F. Giudice and R. Rattazzi, preprint CERN-TH-97-380, [hep-ph/9801271](#), and references therein.
- [43] D. R. Stump, M. Wiest, and C. P. Yuan, Phys. Rev. **D54**, 1936 (1996), [hep-ph/9601362](#); S. Dimopoulos, M. Dine, S. Raby, and S. Thomas, Phys. Rev. Lett. **76**, 3494 (1996), [hep-ph/9601367](#); K. S. Babu, C. Kolda, and F. Wilczek, Phys. Rev. Lett. **77**, 3070 (1996), [hep-ph/9605408](#); S. Dimopoulos, M. Dine, S. Raby, S. Thomas, and J. Wells, Nucl. Phys. Proc. Suppl. A **52** 38 (1997), [hep-ph/9607450](#); S. Dimopoulos, S. Thomas, and J. D. Wells, Phys. Rev. **D54**, 3283 (1996), [hep-ph/9604452](#); Nucl. Phys. **B488**, 39 (1997), [hep-ph/9609434](#); S. Ambrosanio, G. L. Kane, G. D. Kribs, S. P. Martin, and S. Mrenna, Phys. Rev. Lett. **76**, 3498 (1996), [hep-ph/9602239](#); Phys. Rev. **D54**, 5396 (1996); [hep-ph/9605398](#); J. Bagger, K. Matchev, D. Pierce and R.-J. Zhang, Phys. Rev. **D55**, 3188 (1997), [hep-ph/9609444](#); S. Ambrosanio, G. D. Kribs, and S. P. Martin, Phys. Rev. **D56**, 1761 (1997), [hep-ph/9703211](#); H. Baer, M. Brhlik, C.-H. Chen and X. Tata, Phys. Rev. **D55**, 4463 (1998), [hep-ph/9706509](#); C.-H. Chen and J. Gunion, Phys. Rev. **D58**, 075005 (1998), [hep-ph/9802252](#); K.T. Matchev and S. Thomas, preprint FERMILAB-PUB-99-140-T, [hep-ph/9908482](#).
- [44] D. E. Kaplan, F. Lepeintre, A. Masiero, A. E. Nelson and A. Riotto, Phys. Rev. **D60**, 055003 (1999), [hep-ph/9806430](#); H. Cheng, B.A. Dobrescu and K.T. Matchev, Phys. Lett. **B439**, 301 (1998), [hep-ph/9807246](#); Nucl. Phys. **B543**, 47 (1999), [hep-ph/9811316](#); P. Langacker, N. Polonsky and J. Wang, preprint UPR-844-T, [hep-ph/9905252](#); D.E. Kaplan and G.D. Kribs, preprint UW-PT-99-12, [hep-ph/9906341](#).
- [45] M. Dine, Y. Nir and Y. Shirman, Phys. Rev. **D55**, 1501 (1997), [hep-ph/9607397](#); T. Han and R. Zhang, Phys. Lett. **B428**, 120 (1998), [hep-ph/9802422](#).
- [46] C. Chou and M.E. Peskin, [hep-ph/9909536](#).
- [47] U. Sarid and S. Thomas, preprint UND-HEP-98-US01, [hep-ph/9909349](#).

- [48] A. Bartl, W. Porod, M.A. Garcia-Jareno, M.B. Magro, J.W. Valle and W. Majerotto, Phys. Lett. **B384**, 151 (1996), [hep-ph/9606256](#); M. A. Diaz, D. A. Restrepo and J W. F. Valle, preprint FTUV/99-25, [hep-ph/9908286](#); F. de Campos *et al.*, [hep-ph/9903245](#).
- [49] See, e.g. E. L. Berger, B. W. Harris and Z. Sullivan, preprint ANL-HEP-PR-99-05, [hep-ph/9903549](#).
- [50] C. Boehm, A. Djouadi and Y. Mambrini, preprint PM-99-29, [hep-ph/9907428](#).
- [51] R. Barate *et al.* [ALEPH Collaboration], Phys. Lett. **B434**, 189 (1998), [hep-ex/9810028](#); M. Acciarri *et al.* [L3 Collaboration], Phys. Lett. **B445**, 428 (1999); K. Ackerstaff *et al.* [OPAL Collaboration], Eur. Phys. J. **C6**, 225 (1999), [hep-ex/9808026](#).